

Supplemental Data for

**Regularizing firing patterns of rat subthalamic neurons ameliorates
parkinsonian motor deficits**

Qian-Xing Zhuang,¹ Guang-Ying Li,¹ Bin Li,¹ Chang-Zheng Zhang,¹ Xiao-Yang Zhang,¹ Kang Xi,¹
Hong-Zhao Li,¹ Jian-Jun Wang,^{1,2,*} and Jing-Ning Zhu^{1,2,*}

¹State Key Laboratory of Pharmaceutical Biotechnology and Department of Physiology, School of
Life Sciences, Nanjing University, 163 Xianlin Avenue, Nanjing 210023, China

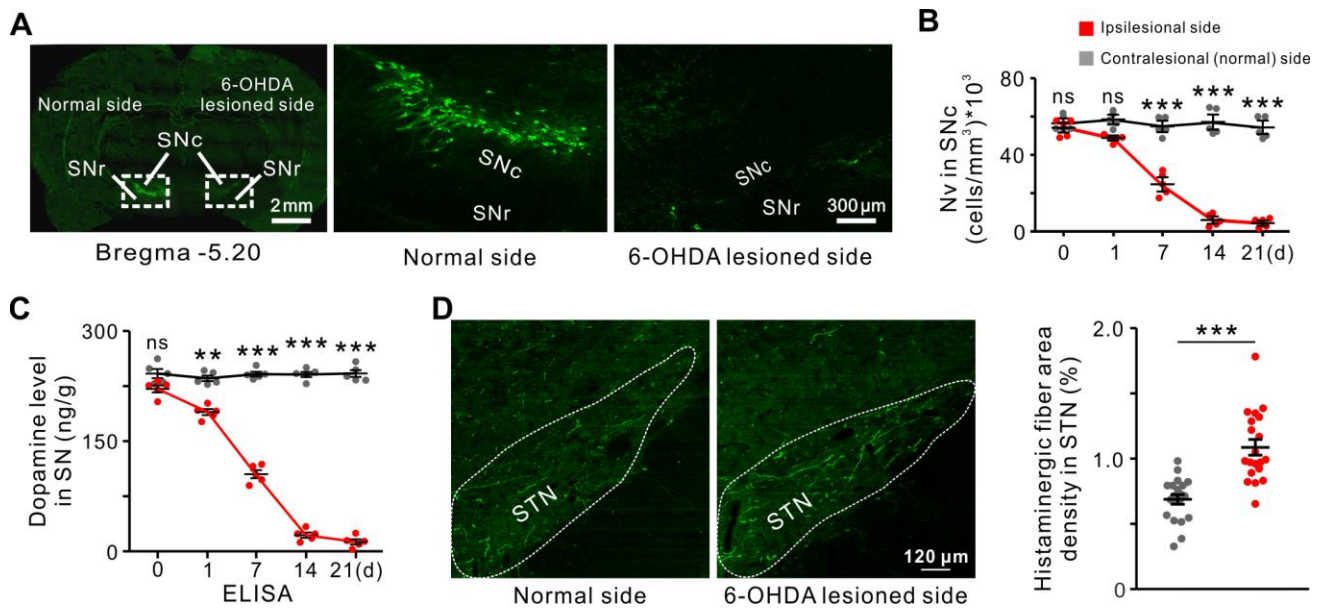
²Institute for Brain Sciences, Nanjing University, 163 Xianlin Avenue, Nanjing 210023, China

*Corresponding authors. Email: jnzhu@nju.edu.cn; jjwang@nju.edu.cn

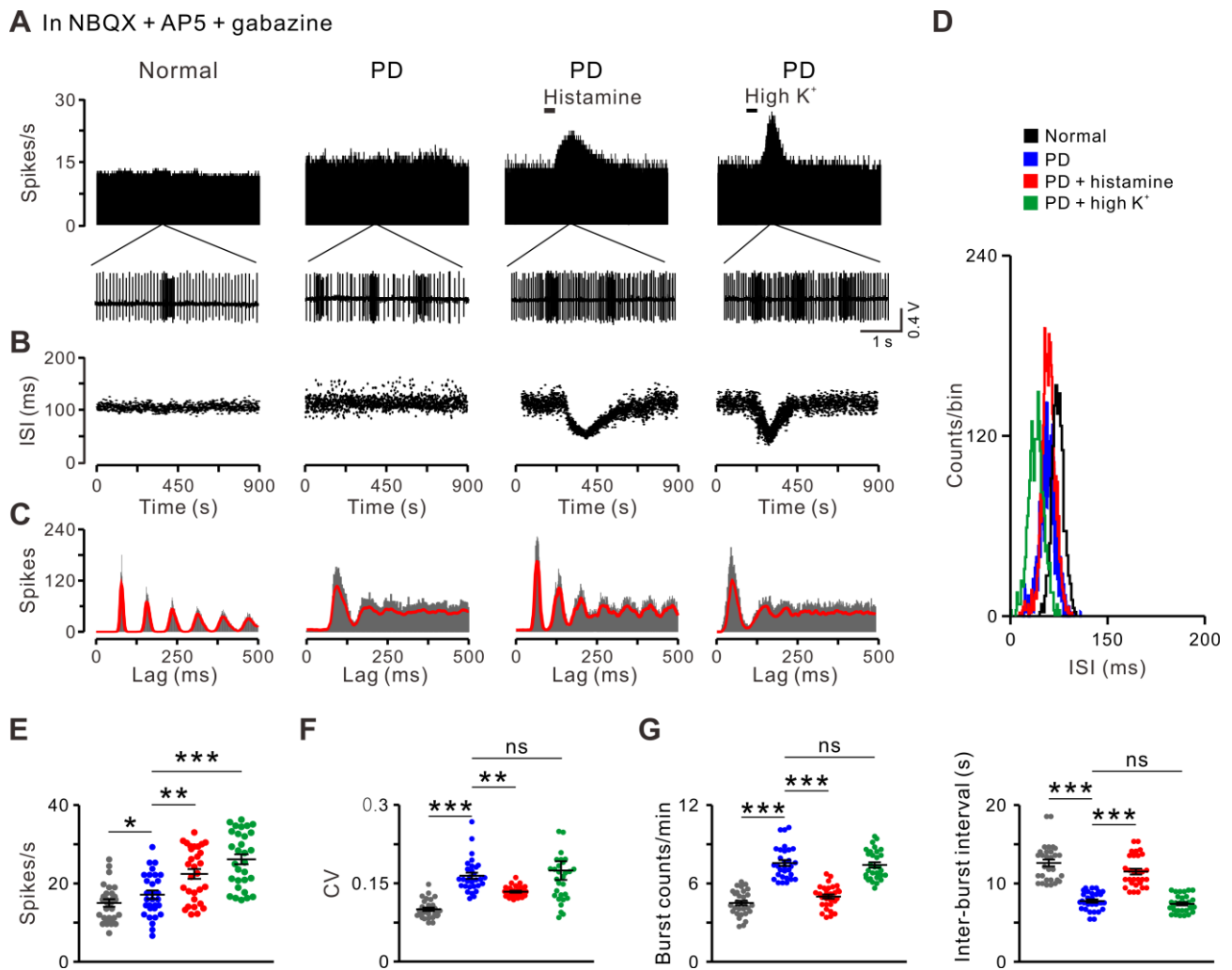
This PDF file includes:

Supplemental Figures 1-15

Supplemental Tables 1-2

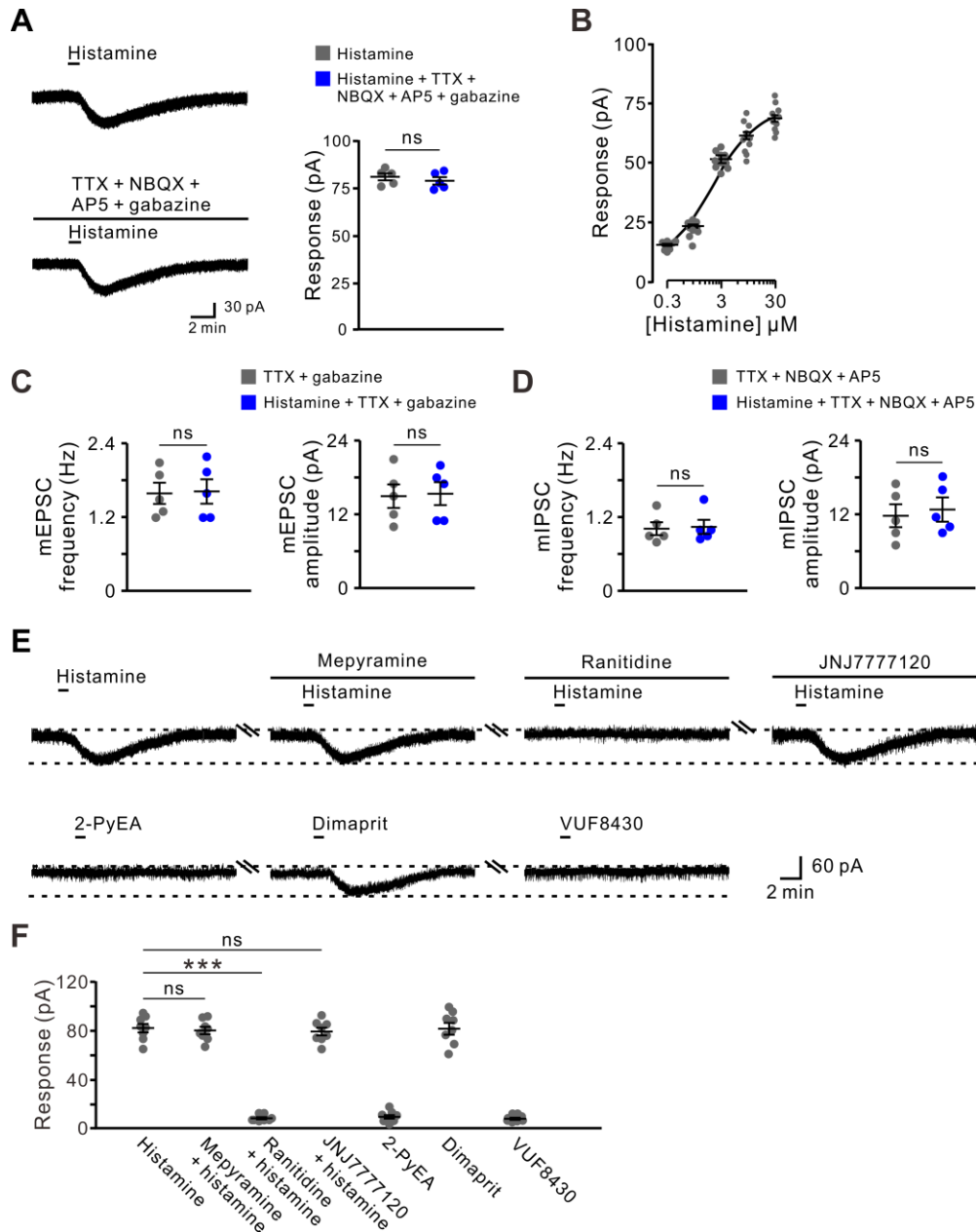


Supplemental Figure 1. Histological identification of the 6-OHDA-lesioned rat model of PD and the altered histaminergic afferents in STN in the pathological process of PD. (A) Antibody staining for tyrosine hydroxylase of a coronal section showing dopaminergic neurons of substantia nigra pars compacta in the normal side of a 6-OHDA-lesioned rat model of PD and the lesion side on 14 days after 6-OHDA injection (3 independent experiments). SNc: substantia nigra pars compacta; SNr: substantia nigra pars reticulata. (B) Numerical density for dopaminergic neurons of substantia nigra pars compacta in the ipsilesional and contralesional sides on 1, 7, 14 and 21 days after 6-OHDA injection ($n = 5$). (C) ELISA analyses show levels of dopamine (ng/g of tissue) in the ipsilesional and contralesional substantia nigra of PD rats ($n = 5$) on 1, 7, 14 and 21 days after 6-OHDA injection. (D) Area density for histaminergic afferent fibers in the ipsilesional and contralesional STNs on 14 days after 6-OHDA injection ($n = 20$). Density was obtained by dividing the area of fibers by the total area examined from 3 independent experiments. Data are represented as mean \pm SEM; ns, no statistical difference, ** $P < 0.01$ and *** $P < 0.001$ by two-way ANOVA with Newman-Keuls post hoc test (B and C) or two-tailed t-test (D).



Supplemental Figure 2. Histamine regularizes firing patterns of STN neurons in PD rats in vitro. (A) Effects of histamine (10 μ M) and high K⁺ (10 mM) on firing rates and firing patterns of two recorded STN neurons in normal and PD rats in the presence of NBQX (20 μ M), AP5 (50 μ M) and gabazine (50 μ M). PSTHs show both histamine and high K⁺ excited the STN neurons in PD rats. Oscilloscope traces show basal firings of STN neurons in normal and PD rats and changes in firings of a STN neuron in response to histamine and high K⁺ in a PD rat. The X-axis scales for PSTHs of (A) shares the X-axis scale bars of (B). (B-D) Scatter plots of ISI series (B), autocorrelation histograms (C) and ISI histograms (D) show that histamine, rather than high K⁺, narrowed ISI distribution and promoted periodicity of STN neuronal firing. (E-G) Histamine increased the firing

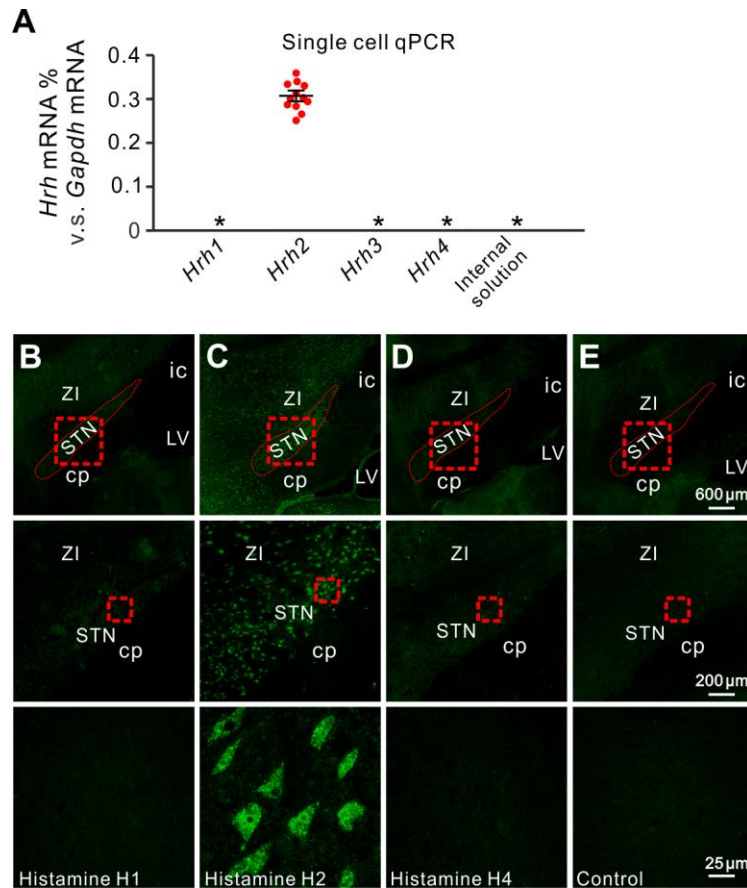
rates (**E**), decreased CV of ISIs (**F**), reduced the number of bursts (**G**, left panel), and prolonged the inter-burst intervals (**G**, right panel) of STN neurons in PD rats ($n = 30$). Data are represented as mean \pm SEM; ns, no statistical difference, * $P < 0.05$, ** $P < 0.01$ and *** $P < 0.001$ by one-way ANOVA with Newman-Keuls post hoc test (**E-G**).



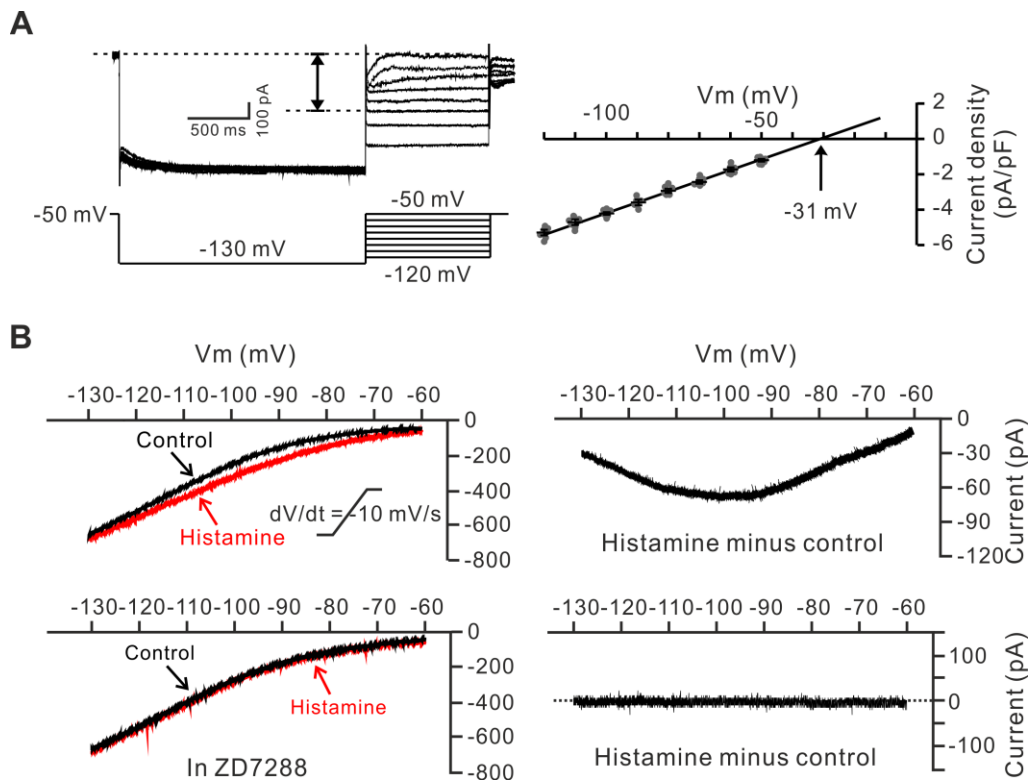
Supplemental Figure 3. Histamine excites STN neurons via postsynaptic histamine H2 receptor.

(A) Patch-clamp recordings on a STN neurons and group data show that TTX (0.3 μ M), NBQX (20 μ M), AP5 (50 μ M) and gabazine (50 μ M) did not block inward currents induced by histamine (10 μ M) on STN neurons ($n = 5$). (B) Concentration-response curves for histamine on the 10 recorded STN neurons show that histamine concentration-dependently excited STN neurons with the mean EC50 of 2.86 μ M. (C and D) Histamine had no effect on the miniature EPSCs (C) and IPSCs (D) on

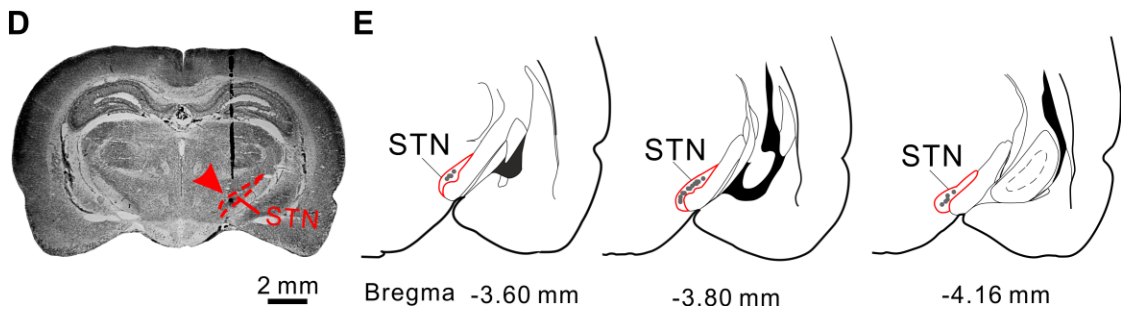
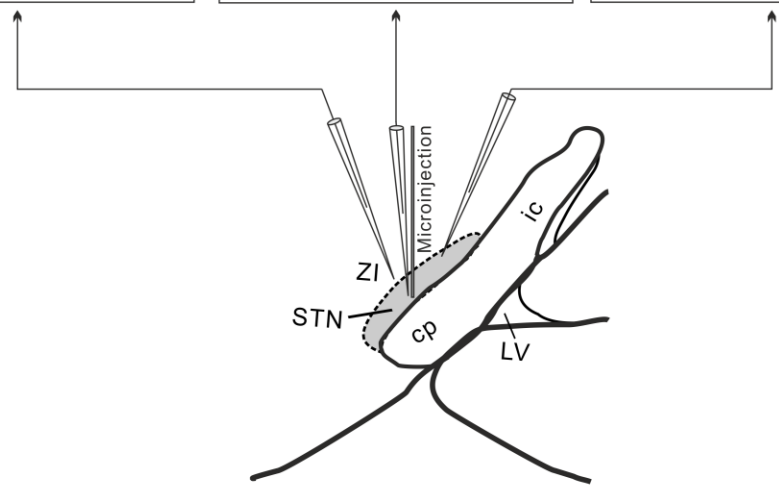
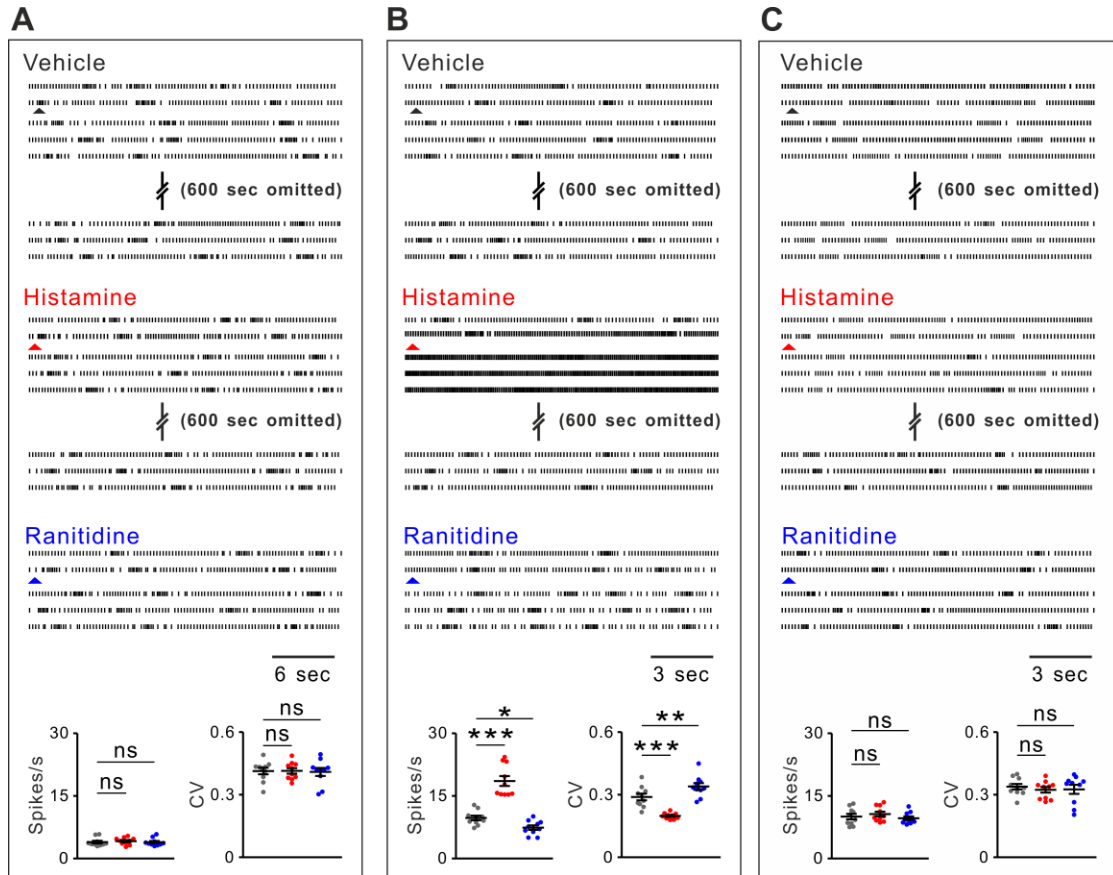
the recorded STN neurons ($n = 5$). **(E)** Effects of histamine H1 receptor selective antagonist mepyramine (1 μM), H2 receptor selective antagonist ranitidine (1 μM) and H4 receptor selective antagonist JNJ777120 (10 μM) on the histamine-induced inward currents on a STN neuron, and the effects of H1 receptor selective agonist 2-pyridylethylamine (2-PyEA, 30 μM), H2 receptor selective agonist dimaprit (30 μM) and H4 receptor selective agonist VUF8430 (30 μM) on the same cell. **(F)** Group data show the effects of histaminergic agents on the tested STN neurons ($n = 8$). Data are represented as mean \pm SEM; ns, no statistical difference, and *** $P < 0.001$ by two-tailed paired t-test (**A**, **C** and **D**) or one-way ANOVA with Newman-Keuls post hoc test (**F**).



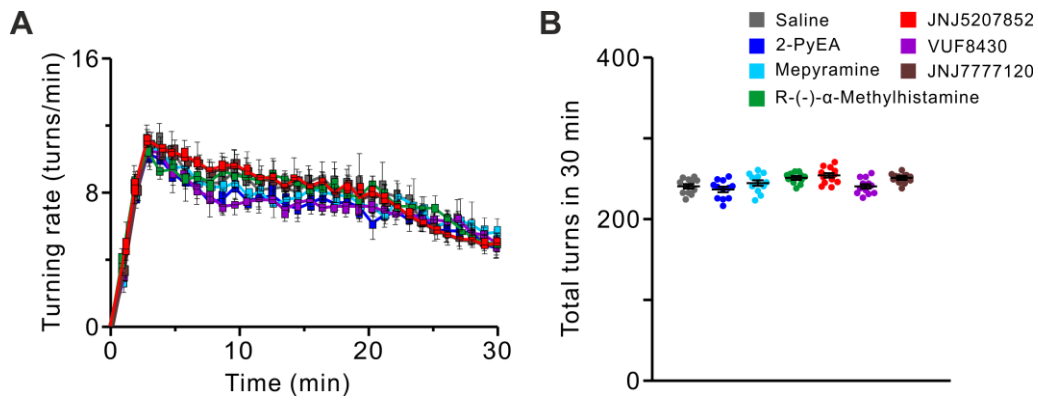
Supplemental Figure 4. Histamine H2 receptor is expressed and distributed in rat STN. (A) Single-cell qPCR showing the expression of histamine H1, H2, H3 and H4 receptor mRNAs in the rat STN. Of the tested 12 cells, all (12/12, 100%) expressed detectable levels of H2 receptor mRNA. Asterisks indicate samples showing no specific signal. Internal solution of the pipettes using in patch clamp recordings served as negative control. (B-E) Antibody staining for postsynaptic H1 (B), H2 (C) and H4 (D) receptors in the STN (3 independent experiments). Negative staining control (E) by omitting the primary antiserum. cp, cerebral peduncle; ic, internal capsule; LV, lateral ventricle; ZI, zona incerta. Data are represented as mean \pm SEM.



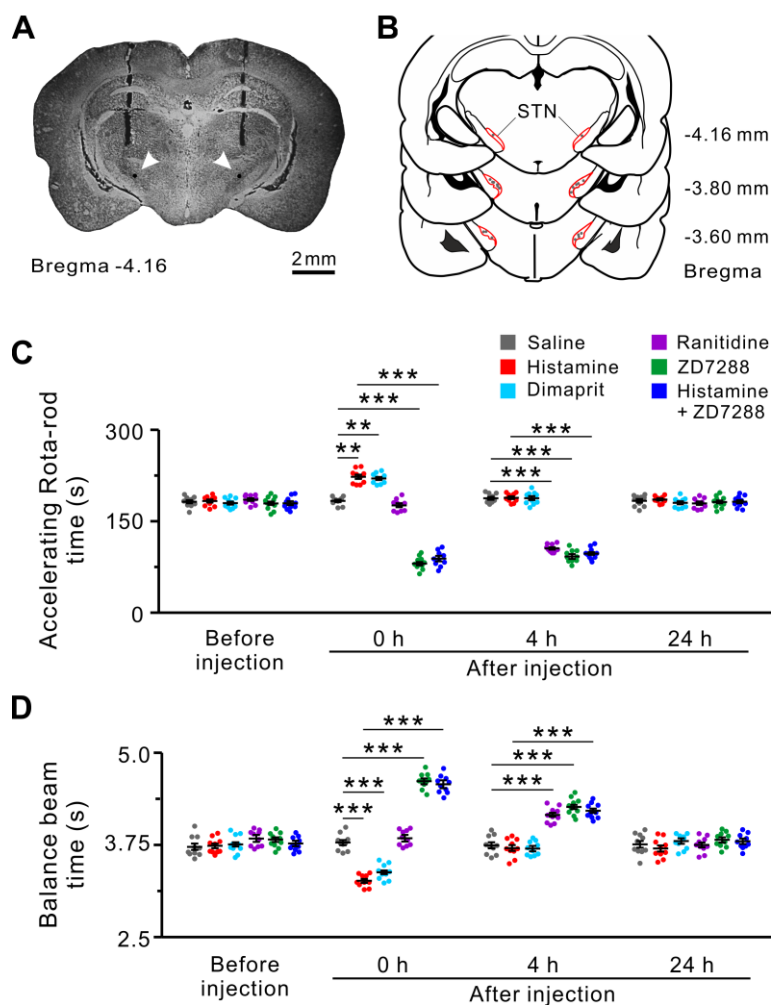
Supplemental Figure 5. The electrophysiological feature of HCN channel and its inward current induced by histamine on STN neurons. (A) The reversal potential of the hyperpolarization-activated (HCN) current was determined by clamping the recorded STN neuron to -130 mV for 2 s and then depolarizing it in 10 mV at 1 s increments to -50 mV. The mean recorded tail currents of HCN (the double-headed arrow in the left panel indicates the measure at -100 mV) were plotted against membrane potentials, and a linear regression was performed ($n = 6$). The reversal potential of the HCN current was about -31 mV. (B) The histamine-induced changes in I - V curves in the absence and presence of ZD7288 (50 μ M). The difference current representing the histamine-induced current shown in the right panel exhibited a hyperpolarization-activated feature of HCN current, and totally blocked by ZD7288. Data are represented as mean \pm SEM.



Supplemental Figure 6. Functional and histological identification of microinjection of the histaminergic agents in the STN of PD rats. (A-C) Raster plots showed unitary activity of STN neurons continuously recorded in vivo before and after microinjection of vehicle, histamine (1 μ g) and ranitidine (3.5 μ g). Neurons in the border between STN and zona incerta (A and C, $n = 10$, respectively) did not exhibit any changes in firing rate and firing pattern following vehicle, histamine and ranitidine microinjections, whereas neurons recorded close to the injecting site (B) within the STN exhibited a significant response to injection of histamine or ranitidine rather than vehicle ($n = 10$). Note that the spontaneous firing rate of zona incerta neurons (A) is significantly lower than that of STN neurons (B and C) and histamine increased the firing rate and decreased CV of ISIs, while ranitidine decreased the firing rate and increased CV of ISIs on STN neurons (B). cp, cerebral peduncle; ic, internal capsule; LV, lateral ventricle; ZI, zona incerta. (D) A coronal section (80 μ m in thickness) showing the site of ipsilesional microinjection within the STN (indicated by the arrowhead). The trace of guide tube shows that the lower end of tube was positioned 1.8 mm above the STN. (E) Histological reconstruction showing the microinjection sites across 22 animals. Data are represented as mean \pm SEM; ns, no statistical difference, * $P < 0.05$, ** $P < 0.01$ and *** $P < 0.001$ by one-way ANOVA with Newman-Keuls post hoc test (A-C).

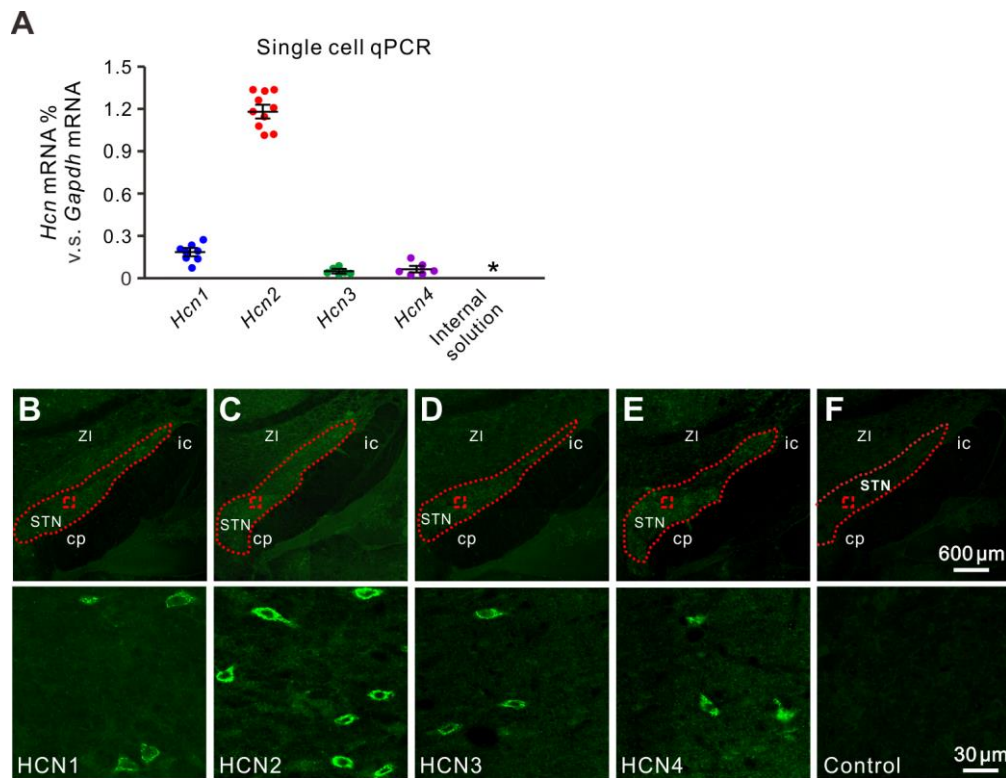


Supplemental Figure 7. Effects of histamine H1, H3 and H4 receptor agonists and antagonists on turning behavior of PD rats. Microinjection of 2-PyEA (selective agonist for H1 receptor; 1 μ g), mepyramine (selective antagonist for H1 receptor; 4 μ g), R-(-)- α -Methylhistamine (selective agonist for H3 receptor; 1.5 μ g), JNJ5207852 (selective antagonist for H3 receptor; 2 μ g), VUF8430 (selective agonist for H4 receptor; 3 μ g), or JNJ7777120 (selective antagonist for H4 receptor; 2.5 μ g) into the STN had no effect on rate (**A**) and cumulative number (**B**) of the apomorphine-induced turnings in PD rats ($n = 12$). Data are represented as median (horizontal bar) with 25th-75th (box) and 5th-95th (whiskers) percentiles or mean \pm SEM, and analyzed by one-way ANOVA with Newman-Keuls post hoc test.

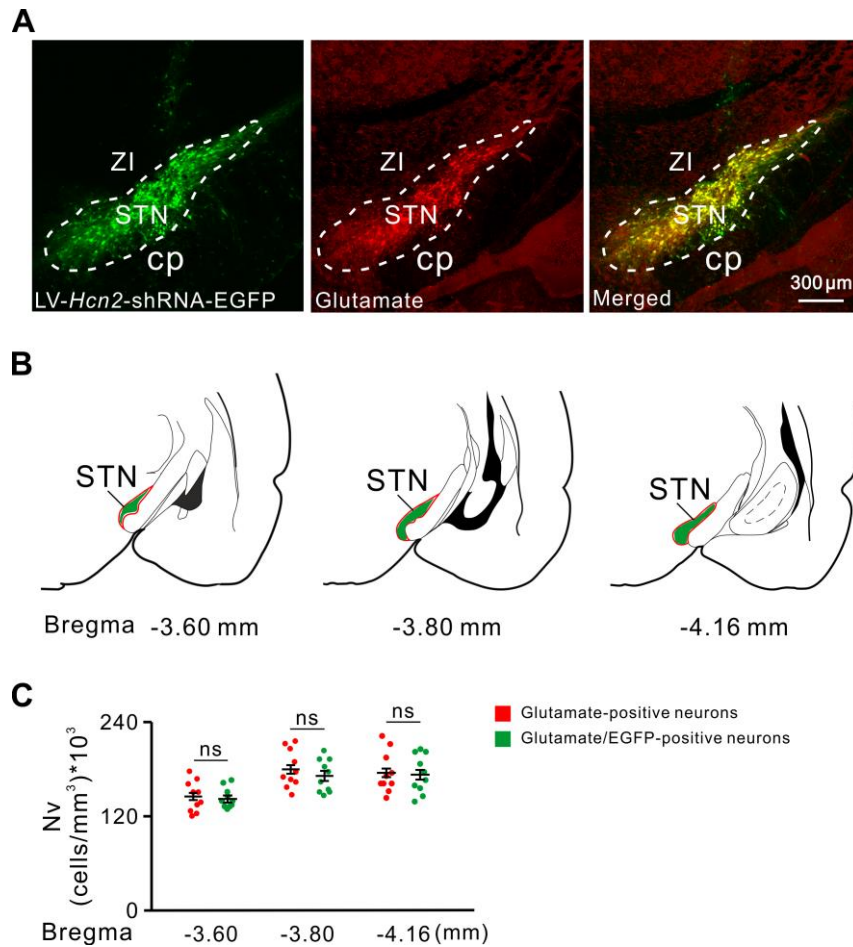


Supplemental Figure 8. Microinjection of histamine into bilateral STNs improves motor performances in normal rats. (A) A coronal section showing the sites of microinjection into bilateral STNs (indicated by arrowheads). The traces of guide tubes show that the lower ends of tubes were positioned 1.8 mm above bilateral STNs. (B) Histological reconstruction showing the microinjection sites in bilateral STNs across 10 animals. (C and D) Effects of microinjection of histaminergic agents into bilateral STNs on motor performances of normal rats in accelerating rota-rod (C) and balance beam (D) tests. Histamine and dimaprit (selective agonist for H2 receptor) significantly promoted motor performances in rota-rod and balance beam, whereas blockage of endogenous histaminergic inputs by ranitidine (selective antagonist for H2 receptor) and ZD7288

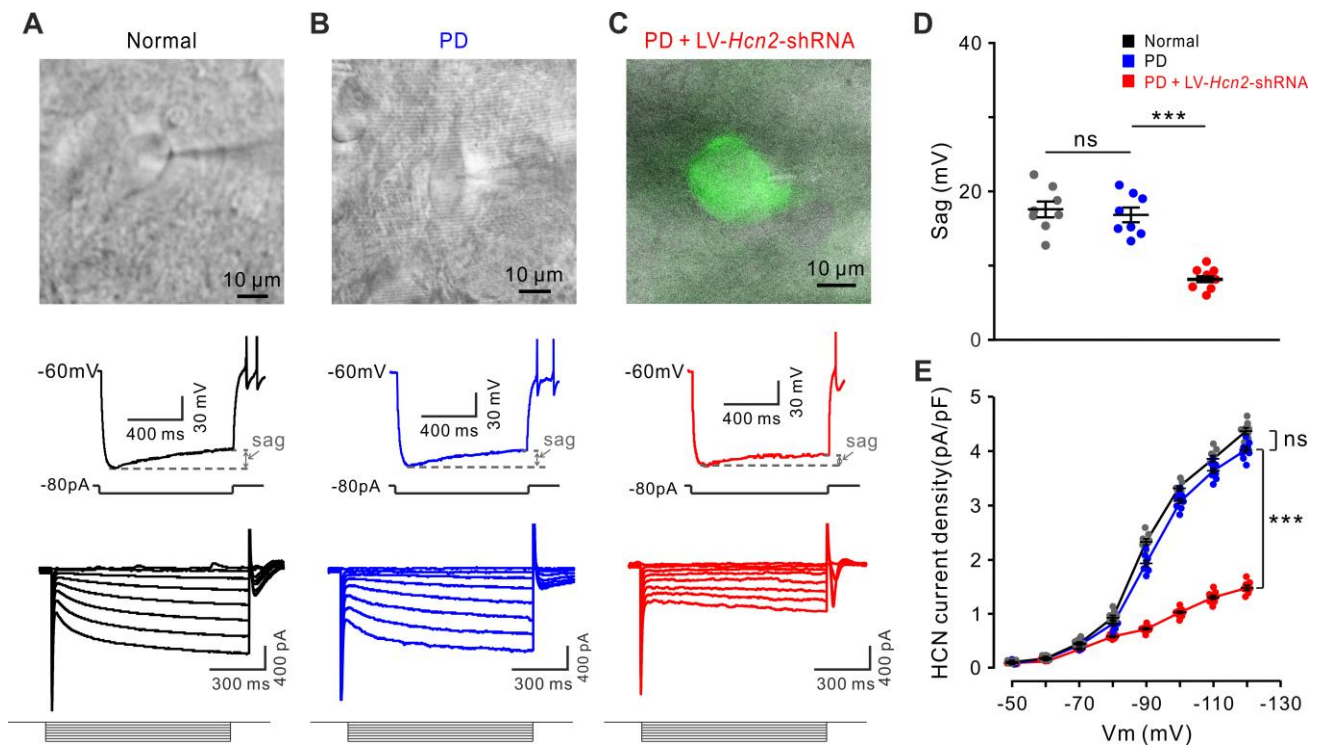
(selective blocker for HCN channel) attenuated motor performances. ZD7288 also blocked the histamine-induced improvements in motor performances ($n = 10$). Data are represented as mean \pm SEM; ** $P < 0.01$ and *** $P < 0.001$ by repeated measures two-way ANOVA with Newman-Keuls post hoc test.



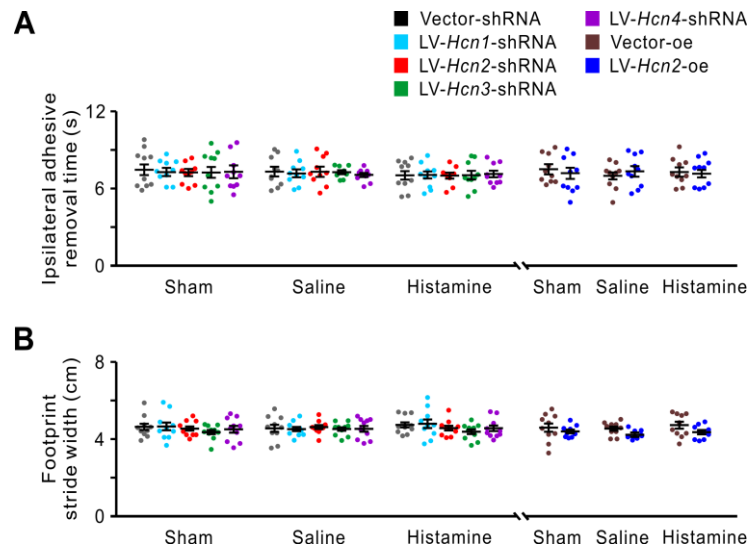
Supplemental Figure 9. The distribution and expression of four HCN channel subtypes (HCN1-4) in rat STN. (A) Single-cell qPCR showing relative expression of *Hcn1*, *Hcn2*, *Hcn3* and *Hcn4* mRNAs in the STN. Of the tested 12 cells, 8 (66.7%) expressed detectable levels of *Hcn1* mRNA, 10 (83.3%) expressed *Hcn2* mRNA, 6 (50%) expressed *Hcn3* mRNA and 6 (50%) expressed *Hcn4* mRNA. Asterisks indicate samples showing no specific signal. Internal solution of the pipettes using in patch clamp recordings served as negative control. (B-F) Antibody staining for HCN1 (B), HCN2 (C), HCN3 (D) and HCN4 (E) channel subtypes in the rat STN (3 independent experiments). Negative staining control (F) by omitting the primary antiserum. cp, cerebral peduncle; ic, internal capsule; ZI, zona incerta. Data are represented as mean \pm SEM.



Supplemental Figure 10. Mapping LV-*Hcn2*-shRNA expression in the rat STN neurons. (A) Coronal sections showing LV-*Hcn2*-shRNA (EGFP-positive) expression in the STN glutamatergic neurons (3 independent experiments). (B) Illustration of lentivirus transgene expression in rat STN from Bregma -3.60 to -4.16 mm at 21 day post lentivirus injection. EGFP expression in soma was observed (as shown in A) and illustrated with green shading, and EGFP-positive neurons were restricted to the STN area. (C) Numerical density for the glutamate-positive neurons and the glutamate/EGFP-positive neurons in the STN from Bregma -3.60 to -4.16 mm at 21 day post lentivirus injection ($n = 10$). Data are represented as mean \pm SEM; ns, no statistical difference by two-way ANOVA with Newman-Keuls post hoc test.

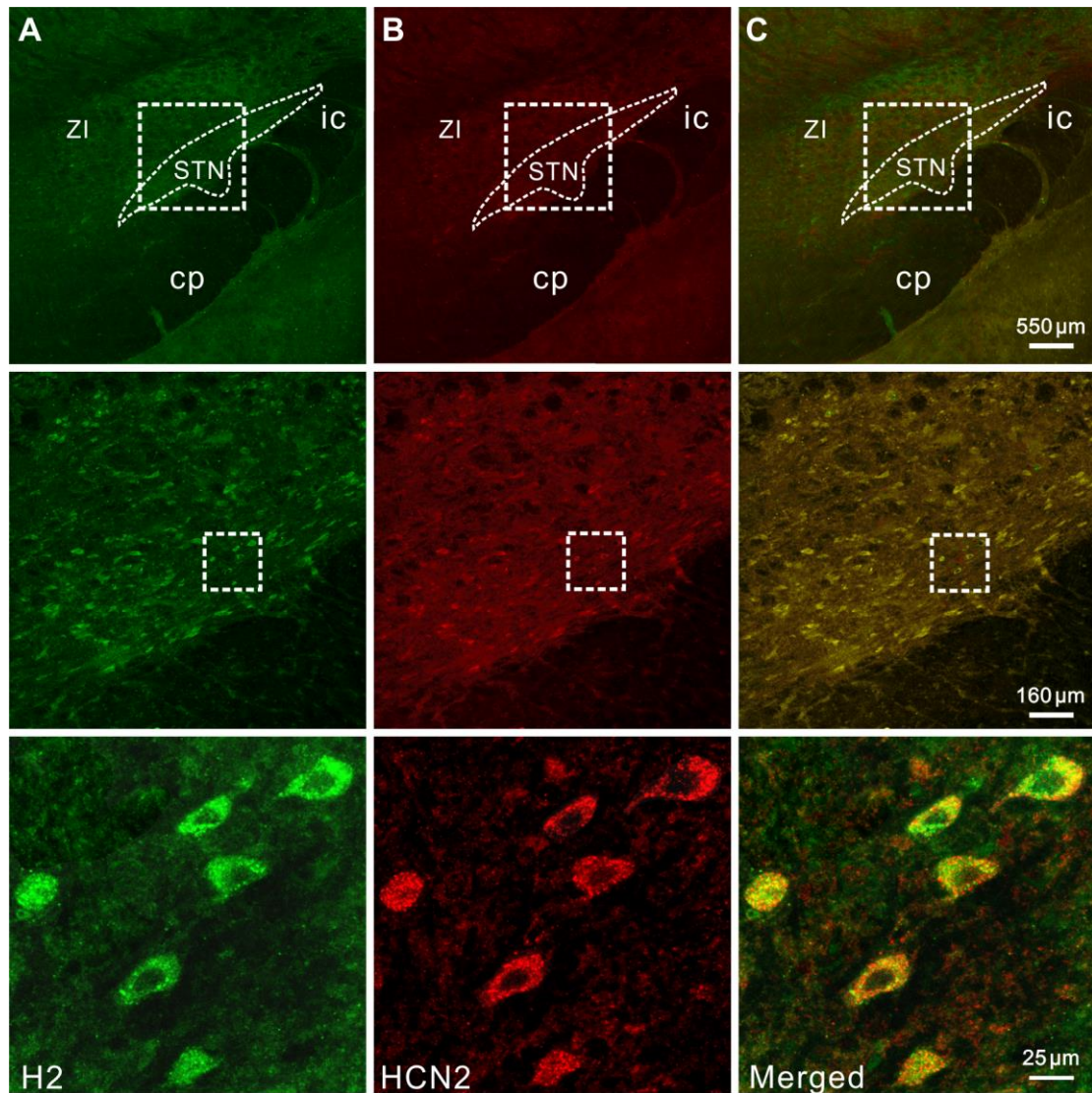


Supplemental Figure 11. A decrease in HCN channel activity in the STN neurons after downregulation of HCN2 subtypes. (A-C) The depolarizing voltage sag in response to an 80 pA hyperpolarizing current pulse and a series of 1 s hyperpolarizing voltage steps (ranging from -50 to -120 mV in 10 mV steps) on the recorded STN neurons from normal (A), PD (B) and PD with HCN2 downregulation (C) rats. (D) Group data show the depolarizing voltage sag on the recorded STN neurons ($n = 8$). (E) Plots of HCN current density on the recorded STN neurons ($n = 8$). Data are represented as mean \pm SEM; ns, no statistical difference, and *** $P < 0.001$ by one-way (D) or two-way ANOVA (E) with Newman-Keuls post hoc test.

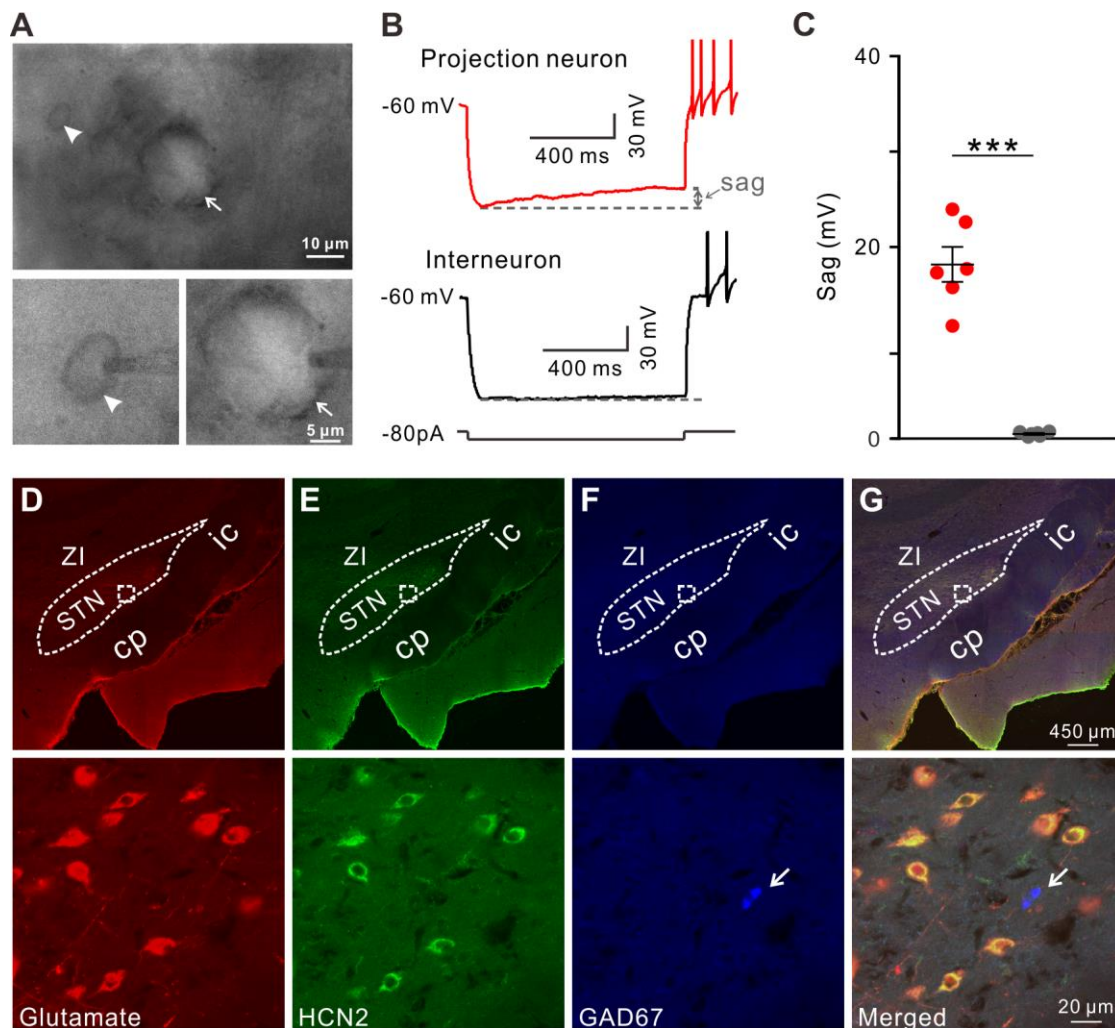


Supplemental Figure 12. Effects of downregulation of HCN1-4 subtypes and upregulation of HCN2 subtype in STN on ipsilesional adhesive removal time and stride width of PD rats. (A) Ipsilateral adhesive removal time ($n = 10$). **(B)** Stride width ($n = 10$). Data are represented as mean \pm SEM, and analyzed by two-way ANOVA with Newman-Keuls post hoc test.

rota-rod and balance beam ($n = 10$). Data are represented as mean \pm SEM; ns, no statistical difference, ** $P < 0.01$ and *** $P < 0.001$ by repeated measures two-way ANOVA with Newman-Keuls post hoc test.



Supplemental Figure 14. Co-localization of histamine H2 receptor and HCN2 channel in the same STN neurons in the rat. Double immunostaining results show that H2 receptor (**A**) and HCN2 channel (**B**) were not only present in the STN but also co-localized (**C**) in the same STN neuron of the rat (3 independent experiments). cp, cerebral peduncle; ic, internal capsule; ZI, zona incerta.



Supplemental Figure 15. Selective expression and localization of HCN2 channel in the glutamatergic projection neurons in the STN. (A and B) The recorded neurons with the diameter larger than 20 μm (indicated by arrows, presumably glutamatergic projection neurons), instead of ones with the diameter smaller than 10 μm (indicated by arrowheads, presumably GABAergic interneurons), exhibit depolarization sag, a hallmark of HCN channel. (C) Group data show the depolarization sag of the recorded projection neurons and interneurons ($n = 6$, respectively). (D-G) Triple immunostaining results show the presence of HCN2 channel (E) in the glutamatergic (D) rather than GABAergic neurons (F) in the STN (3 independent experiments). cp, cerebral peduncle; ic, internal capsule; ZI, zona incerta. Data are represented as mean \pm SEM; *** $P < 0.001$ by two-tailed t-test.

Supplemental Table 1. Sequences of oligonucleotide primers used for PCR amplification.

Primers	Sequences (5'-3')	Sources
<i>Hcn1p1</i>	ATGCCTCTCTTTGCTAACGC	NM_053375
<i>Hcn1p2</i>	TATTCCTCCAAGACCTCGTTGAA	
<i>Hcn2p1</i>	CTACAGCGACTTCAGGTTCTACTGGG	NM_053684
<i>Hcn2p2</i>	GACCACGTTGAAGACGATCCAGG	
<i>Hcn3p1</i>	GTCGGAGAACAGCCAGTGTA	NM_053685
<i>Hcn3p2</i>	TGAGCGTCTAGCAGATCGAG	
<i>Hcn4p1</i>	ATCAACGGCATGGTGAATAACTC	NM_021658
<i>Hcn4p2</i>	TGCCCTGGTAGCGGTGTTC	
<i>Gapdhp1</i>	GAACGGGAAGCTCACTGG	NM_017008
<i>Gapdhp2</i>	GCCTGCTTCACCACCTTCT	

Supplemental Table 2. Statistical report for each experiment.

Figure panel	Test used	N value	Statistical result
Figure 1B	Two-way ANOVA	5	HPLC: group, $F_{1,40} = 265.756$, $P < 0.001$; time, $F_{4,40} = 18.33$, $P < 0.001$; interaction, $F_{4,40} = 20.928$, $P < 0.001$. ELISA: group, $F_{1,40} = 238.43$, $P < 0.001$; time, $F_{4,40} = 17.205$, $P < 0.001$; interaction, $F_{4,40} = 16.088$, $P < 0.001$.
Figure 1D	One-way ANOVA	12	$F_{2,33} = 692.3$, $P < 0.001$.
Figure 2G	Two-way ANOVA	30	group, $F_{1,232} = 73.813$, $P < 0.001$; treatment, $F_{3,232} = 117.576$, $P < 0.001$; interaction, $F_{3,232} = 1.054$, $P = 0.373$.
Figure 2H	Two-way ANOVA	15	group, $F_{1,112} = 172.576$, $P < 0.001$; treatment, $F_{3,112} = 18.106$, $P < 0.001$; interaction, $F_{3,112} = 1.2$, $P = 0.313$.
Figure 2I	Two-way ANOVA	15	Burst counts: group, $F_{1,112} = 1202.892$, $P < 0.001$; treatment, $F_{3,112} = 56.794$, $P < 0.001$; interaction, $F_{3,112} = 18.434$, $P < 0.001$. Inter-burst intervals: group, $F_{1,112} = 952.403$, $P < 0.001$; treatment, $F_{3,112} = 48.47$, $P < 0.001$; interaction, $F_{3,72} = 3.477$, $P = 0.018$.
Figure 3B	Two-tailed paired t-test	5	At -90 mV: $T = 7.716$, $df = 4$, $P < 0.001$. At -100 mV: $T = 7.720$, $df = 4$, $P < 0.001$. V₁₂: $T = 2.963$, $df = 4$, $P = 0.0414$.
Figure 3C	One-way ANOVA	8	$F_{3,28} = 347.3$, $P < 0.001$.
Figure 3D	One-way ANOVA	8	$F_{2,21} = 445$, $P < 0.001$.
Figure 3G	One-way ANOVA	30	$F_{5,174} = 104.198$, $P < 0.001$.
Figure 4A	One-way ANOVA	12	$F_{5,66} = 722.872$, $P < 0.001$.
Figure 4B	Two-way ANOVA	10	group, $F_{1,108} = 845.505$, $P < 0.001$; treatment, $F_{5,108} = 65.429$, $P < 0.001$; interaction, $F_{5,108} = 58.97$, $P < 0.001$.
Figure 4C (Stride length)	Two-way ANOVA	10	group, $F_{1,108} = 0.283$, $P = 0.596$; treatment, $F_{5,108} = 154.93$, $P < 0.001$; interaction, $F_{5,108} = 0.0434$, $P = 0.999$.
Figure 4C (stride width)	One-way ANOVA	10	$F_{5,54} = 1.344$, $P = 0.26$.
Figure 5A	One-way ANOVA	6	mRNAs: $F_{2,15} = 171.8$, $P < 0.001$. Proteins: $F_{2,15} = 174.7$, $P < 0.001$.
Figure 5B	One-way ANOVA	6	mRNAs: $F_{2,15} = 157.8$, $P < 0.001$. Proteins: $F_{2,15} = 325.8$, $P < 0.001$.
Figure 5C	One-way ANOVA	6	mRNAs: $F_{2,15} = 147.7$, $P < 0.001$. Proteins: $F_{2,15} = 540.8$, $P < 0.001$.

Figure panel	Test used	N value	Statistical result
Figure 5D	One-way ANOVA	6	mRNAs: $F_{2,15} = 118, P < 0.001$. Proteins: $F_{2,15} = 108.1, P < 0.001$.
Figure 5E	One-way ANOVA	6	mRNAs: $F_{2,15} = 79.85, P < 0.001$. Proteins: $F_{2,15} = 426.3, P < 0.001$.
Figure 5F (downregulation)	Two-way ANOVA	12	group, $F_{2,165} = 1748.2, P < 0.001$; treatment, $F_{4,165} = 2944.6, P < 0.001$; interaction, $F_{8,165} = 105, P < 0.001$.
Figure 5F (upregulation)	Two-way ANOVA	12	group, $F_{2,66} = 1034.9, P < 0.001$; treatment, $F_{1,66} = 852.79, P < 0.001$; interaction, $F_{2,66} = 1.056, P = 0.354$
Figure 5G (downregulation)	Two-way ANOVA	10	group, $F_{2,135} = 59.797, P < 0.001$; treatment, $F_{4,135} = 35.88, P < 0.001$; interaction, $F_{8,135} = 2.73, P = 0.008$.
Figure 5G (upregulation)	Two-way ANOVA	10	group, $F_{2,54} = 63.267, P < 0.001$; treatment, $F_{1,54} = 42.703, P < 0.001$; interaction, $F_{2,54} = 0.481, P = 0.621$.
Figure 5H (downregulation)	Two-way ANOVA	10	Ipsilesional: group, $F_{2,135} = 35.104, P < 0.001$; treatment, $F_{4,135} = 28.697, P < 0.001$; interaction, $F_{8,135} = 1.76, P = 0.09$. Contralesional: group, $F_{2,135} = 37.383, P < 0.001$; treatment, $F_{4,135} = 23.291, P < 0.001$; interaction, $F_{8,135} = 1.669, P = 0.111$.
Figure 5H (upregulation)	Two-way ANOVA	10	Ipsilateral: group, $F_{2,54} = 24.743, P < 0.001$; treatment, $F_{1,54} = 18.308, P < 0.001$; interaction, $F_{2,54} = 0.108, P = 0.898$. Contralateral: group, $F_{2,54} = 23.62, P < 0.001$; treatment, $F_{1,54} = 18.085, P < 0.001$; interaction, $F_{2,54} = 0.233, P = 0.793$.
Figure 6E	One-way ANOVA	30	$F_{2,87} = 442.4, P < 0.001$.
Figure 6F	One-way ANOVA	15	Burst counts: $F_{2,42} = 620.9, P < 0.001$. Inter-burst interval: $F_{2,42} = 232.8, P < 0.001$.
Figure 6K	One-way ANOVA	25	$F_{2,72} = 102.6, P < 0.001$
Figure 6L	One-way ANOVA	15	Burst counts: $F_{2,42} = 98.6, P < 0.001$. Inter-burst interval: $F_{2,42} = 77.28, P < 0.001$.
Figure 7A	One-way ANOVA	5	$F_{2,12} = 14.031, P < 0.001$.
Figure 7B	Two-tailed paired t-test	7	$T = 7.059, df = 12, P < 0.001$.
Figure 7G	One-way ANOVA	15	$F_{2,42} = 100.1, P < 0.001$.
Figure 7H	One-way ANOVA	15	Burst counts: $F_{2,42} = 244.4, P < 0.001$. Inter-burst interval: $F_{2,42} = 135.9, P < 0.001$.
Figure 7J	One-way ANOVA	15	$F_{2,42} = 99.7, P < 0.001$.
Supplemental Figure 1B	Two-way ANOVA	5	group, $F_{1,40} = 583.153, P < 0.001$; time, $F_{4,40} = 91.911, P < 0.001$; interaction, $F_{4,40} = 83.605, P < 0.001$.
Supplemental	Two-way	5	group, $F_{1,40} = 1101.52, P < 0.001$; time, $F_{4,40} = 156.572, P <$

Figure panel	Test used	N value	Statistical result
Figure 1C	ANOVA		0.001; interaction, $F_{4,40} = 165.501$, $P < 0.001$.
Supplemental	Two-tailed	20	$T = 5.660$, $df = 38$, $P < 0.001$.
Figure 1D	t-test		
Supplemental	One-way	30	$F_{3,116} = 15.21$, $P < 0.001$.
Figure 2E	ANOVA		
Supplemental	One-way	30	$F_{3,116} = 10.26$, $P < 0.001$.
Figure 2F	ANOVA		
Supplemental	One-way	30	Burst counts: $F_{3,116} = 53.78$, $P < 0.001$.
Figure 2G	ANOVA		Inter-burst intervals: $F_{3,116} = 52.32$, $P < 0.001$.
Supplemental	Two-tailed	5	$T = 0.642$, $df = 4$, $P = 0.5558$.
Figure 3A	paired t-test		
Supplemental	Two-tailed	5	Frequency: $T = 0.802$, $df = 4$, $P = 0.468$.
Figure 3C	paired t-test		Amplitude: $T = 0.667$, $df = 4$, $P = 0.541$.
Supplemental	Two-tailed	5	Frequency: $T = 0.688$, $df = 4$, $P = 0.529$.
Figure 3D	paired t-test		Amplitude: $T = 1.826$, $df = 4$, $P = 0.142$.
Supplemental	One-way	8	$F_{3,28} = 139.6$, $P < 0.001$.
Figure 3F	ANOVA		
Supplemental	One-way	10	Firing rate: $F_{2,27} = 0.232$, $P = 0.795$.
Figure 6A	ANOVA		CV of ISIs: $F_{2,27} = 0.0287$, $P = 0.972$.
Supplemental	One-way	10	Firing rate: $F_{2,27} = 52.601$, $P < 0.001$.
Figure 6B	ANOVA		CV of ISIs: $F_{2,27} = 34.352$, $P < 0.001$.
Supplemental	One-way	10	Firing rate: $F_{2,27} = 0.834$, $P = 0.445$.
Figure 6C	ANOVA		CV of ISIs: $F_{2,27} = 0.24$, $P = 0.789$.
Supplemental	One-way	12	$F_{6,77} = 1.575$, $P = 0.166$.
Figure 7	ANOVA		
Supplemental	Repeated	10	treatment, $F_{5,54} = 187.352$, $P < 0.001$; time, $F_{3,162} = 41$, $P < 0.001$; interaction, $F_{15,162} = 87.811$, $P < 0.001$.
Figure 8C	measures two-way ANOVA		
Supplemental	Repeated	10	treatment, $F_{5,54} = 47.322$, $P < 0.001$; time, $F_{3,162} = 21.982$, $P < 0.001$; interaction, $F_{15,162} = 41.537$, $P < 0.001$.
Figure 8D	measures two-way ANOVA		
Supplemental	Two-way	10	group, $F_{2,54} = 169.853$, $P < 0.001$; treatment, $F_{1,54} = 9.209$, $P = 0.004$; interaction, $F_{2,54} = 0.075$, $P = 0.928$.
Figure 10	ANOVA		
Supplemental	One-way	8	$F_{2,21} = 84.381$, $P < 0.001$.
Figure 11D	ANOVA		
Supplemental	Two-way	8	group, $F_{2,168} = 1735.476$, $P < 0.001$; treatment, $F_{7,168} = 1619.975$, $P < 0.001$; interaction, $F_{14,168} = 197.25$, $P < 0.001$.
Figure 11E	ANOVA		
Supplemental	Two-way	10	group, $F_{2,135} = 0.252$, $P = 0.778$; treatment, $F_{4,135} = 0.02$, $P = 0.999$; interaction, $F_{8,135} = 0.022$, $P = 1$.
Figure 12A	ANOVA		
(downregulation)			

Figure panel	Test used	N value	Statistical result
Supplemental Figure 12A (upregulation)	Two-way ANOVA	10	group, $F_{2, 54} = 0.087$, $P = 0.916$; treatment, $F_{1, 54} = 0.01$, $P = 0.99$; interaction, $F_{2, 54} = 0.074$, $P = 0.929$.
Supplemental Figure 12B (downregulation)	Two-way ANOVA	10	group, $F_{2, 135} = 0.242$, $P = 0.786$; treatment, $F_{4, 135} = 0.879$, $P = 0.479$; interaction, $F_{8, 135} = 0.266$, $P = 0.976$.
Supplemental Figure 12B (upregulation)	Two-way ANOVA	10	group, $F_{2, 54} = 0.448$, $P = 0.641$; treatment, $F_{1, 54} = 0.036$, $P = 0.85$; interaction, $F_{2, 54} = 0.062$, $P = 0.94$.
Supplemental Figure 13A	Repeated measures two-way ANOVA	10	treatment, $F_{9, 90} = 426.734$, $P < 0.001$; time, $F_{3, 270} = 142.354$, $P < 0.001$; interaction, $F_{27, 270} = 22.597$, $P < 0.001$.
Supplemental Figure 13B	Repeated measures two-way ANOVA	10	treatment, $F_{9, 90} = 246.981$, $P < 0.001$; time, $F_{3, 270} = 8.272$, $P < 0.001$; interaction, $F_{27, 270} = 1.692$, $P = 0.02$.
Supplemental Figure 13C	Repeated measures two-way ANOVA	10	treatment, $F_{3, 36} = 129.731$, $P < 0.001$; time, $F_{3, 108} = 53.362$, $P < 0.001$; interaction, $F_{9, 108} = 21.653$, $P < 0.001$
Supplemental Figure 13D	Repeated measures two-way ANOVA	10	treatment, $F_{3, 36} = 206.528$, $P < 0.001$; time, $F_{3, 108} = 22.052$, $P < 0.001$; interaction, $F_{9, 108} = 10.623$, $P < 0.001$
Supplemental Figure 15	Two-tailed t-test	6	$T = 15.950$, $df = 14$, $P < 0.001$.